Biocomposites based on bentonite and lecithin: An experimental approach supported by molecular dynamics

Qiang Li, Romain Berraud-Pache, Yongjie Yang, Christelle Souprayen, Maguy Jaber

Biocomposites based on bentonite and Lecithin: an experimental approach supported by molecular dynamics

Qiang Li[a], Romain Berraud-Pache[a], Yongjie Yang[a,b] , Christelle Souprayen[a], Maguy Jaber[a,c*]

[a]*Sorbonne Université, Laboratoire d'Archéologie Moléculaire et Structurale(LAMS), CNRS UMR 8220, Paris, 75005, France*

[b]*School of Geoscience and Surveying Engineering, China University of Mining and Technology, Beijing, 100083, China*

[c]*Institut Universitaire de France*

[*]Corresponding author, e-mail: maguy.jaber@sorbonne-universite.fr

Abstract

Natural bio-surfactants have recently attracted much more attention due to their biodegradability and biocompatibility. They are often associated with clay materials to synthesize organoclays and can therefore be ideal materials for environmentally friendly oil-based drilling fluids. In this study, a bio-organoclay was obtained by modifying bentonite with natural soybean lecithin, and the effects of reaction temperature, time, pH, and lecithin concentration on the properties of modified bentonite were analyzed. Structural insights such as clay properties, intercalation process and lecithin organization were obtained using a large variety of experimental techniques and molecular dynamics simulations. The results of this study suggest that some experimental conditions have an important impact on the basal space of the bentonite. Reaction time and temperature did not have a significant effect on the final

properties of the modified bentonite. However, by increasing the pH of the clay material or with a high concentration of lecithin, the interlayer space fluctuates from 1.21 to 5.96 nm. The lecithin molecules adopt a new spatial conformation in the interlayer space becoming perpendicular to the clay surface, which largely increase the interlayer space.

Graphical abstract

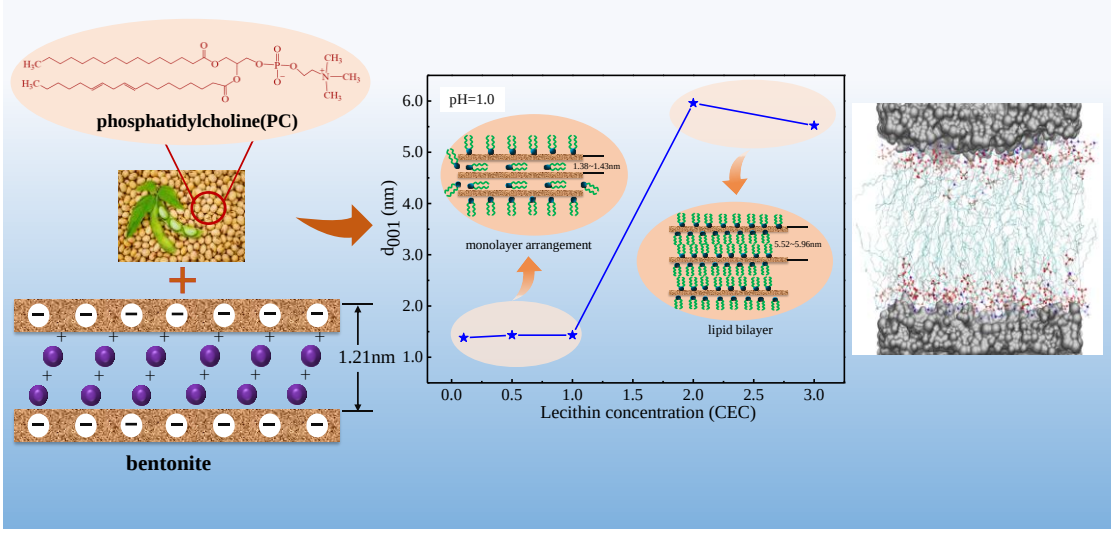

Keywords: organoclay; bentonite; lecithin; bio-surfactant; molecular dynamics

1. Introduction

Clay minerals have been known and applied since antiquity as one of the most important groups of geomaterials. Clay minerals are generally regarded as a group of phyllosilicates whose particles are less than 2 μm. The phyllosilicates structures are based on tetrahedral (T) and octahedral (O) sheet, which can form anisotropic TO or TOT layer in a 1:1 or 2:1 ratio (Bergaya and Lagaly, 2006). Stacking of these layers by van der Waals force or weak dipolar interaction lead to the creation of interlayers space which are occupied by inorganic cations, balancing the charge deficiency caused by isomorphous substitution of the sheets (Xie et al., 2001). Clay minerals

have become essential in modern industry and everyday's life thanks to being abundant, inexpensive and environmentally friendly. In the past two decades, the application of clay minerals in rheological control agents, oil-based drilling fluid, adsorbents of organic pollutants, paints and cosmetics have been widely reported (Li et al., 2021; Lima et al., 2020; Park et al., 2013; Trigueiro et al., 2018; Zhuang et al., 2019). Nowadays, modification of clay minerals has attracted more and more attention (Pereira et al., 2017; Xavier et al., 2016), and the exploration of novel modification methods on clay minerals has never stopped (Zhu et al., 2017).

Bentonite, has gathered considerable research interest due to its availability in mine deposits and soils, nontoxic nature, and high cation exchange capacity (CEC) (Churchman et al., 2006). Montmorillonite (Mt), the main ingredient of bentonite, belongs to the smectite groups where two silica tetrahedral sheets are layered between an alumina octahedral sheet (TOT) (Cui et al., 2014). The montmorillonite layers are negatively charged due to isomorphic substitution(Bergaya, 2013). In general, the aluminum cations in the octahedral sheet is replaced by magnesium ones. Owing to the special properties of montmorillonite, organic modification by exchange the interlayer inorganic cations by organic ones is commonly used to develop organoclays.

In previous studies, quaternary ammonium salts were widely applied in montmorillonite modification and exhibit superior performances in oil-based drilling fluid (Zhuang et al., 2015);(Zhou et al., 2016);(Zhang et al., 2017);(Makhoukhi et al., 2013; Makhoukhi et al., 2016; Xie et al., 2002), notably a better dispersibilty.

Furthermore, the intercalation of oil between the montmorillonite layers induces the layers to swell and exfoliate while the edges and faces of the dispersed layers form a "kind of house-of-cards structure" resulting in a gel system (Agwu et al., 2021). However, the quaternary ammonium salt and quaternary phosphonium salt surfactants usually induce environmental problems due to their toxicity and poor biocompatibility. This limitation restricts their potential use in some application fields (Liu et al., 2017).

In the last few years, there has been a tremendous amount of interest and various efforts regarding the preparation of bio-organoclays to solve the main problems listed above, notably biocompatibility(Biswas et al., 2019). Phospholipids, especially lecithin, have been reported to be good candidates to synthesize bio-organoclays. (Merino et al., 2016) investigated the effect of lecithin concentration and reaction time on modified bentonite and considered that lecithin-bentonites are promising eco-friendly fillers for bio and nanocomposites. (Nagy et al., 2013) studied the adsorption characteristics of nanocomposites containing lecithin and bentonite composite. In addition, the hybrid materials obtained from lecithin-modified clay minerals have received great attention in the fields of biomedicine and pharmaceuticals(Dening et al., 2017; Ruiz-Hitzky et al., 2019; Sabzevari et al., 2022). Phospholipids are a class of lipids constituted of a phosphate polar head-group attached to non-polar hydrocarbon chains. Lecithin is one of the most common phospholipids and mainly composed of phosphatidylcholine (PC) (Cui and Decker, 2016). It can be extracted from vegetables and animal sources such as soybeans, rice beans, sunflower, marine sources, egg yolk, and milk. Lecithin extracted from

soybeans is recognized to be more stable, safer, and affordable from the production point of view(Le et al., 2019). PC contains a choline part, *i.e.* a positively charge trimethyl-amino group, in addition to the negative charge on the phosphate group (Bot et al., 2021). The pKa value of the phosphate group is around 1.5 and it can be protonated at acidic conditions (pH<pKa), which means that the lecithin can exchange interlayer cations in clay minerals.

This publication deals with the preparation of new organoclays based on bentonite and soybean lecithin. The effects of reaction temperature, time, pH, and lecithin concentration on the properties of modified bentonite were analyzed by a variety of characterization techniques such as X-ray diffraction (XRD), Fourier transform infrared (FTIR), Thermogravimetric analyses (TG) and Molecular Dynamics simulations (MD). The interaction between bentonite and lecithin, the intercalation behavior, and the configuration of lecithin in the interlayer space are reported through experiments and molecular dynamics simulations. This study is expected to provide valuable insights into into the preparation of bioorganoclays from lecithin. In addition, some conditions can largely impact the physical properties of the organoclay and help design relevant environmentally-friendly materials.

2 Materials and methods

2.1 Modified bentonite preparation

Bentonite was first pre-swollen in distilled water and stirred for 16h, while lecithin was dissolved in ethanol. The 10 ml of 0.01g/ml bentonite dispersion was added to the 10 ml lecithin solution with different concentrations (0.1~3.0CEC) under constant stirring for 1.0h of contact time. The molecular structure and functional groups of PC ($C_{42}H_{80}NO_8P$, molecular weight=758.06g/mol) are described in Fig. 1. To adjust the pH of the mixture between 1.0 and 9.0, a solution of 6.0 mol/L of HCl

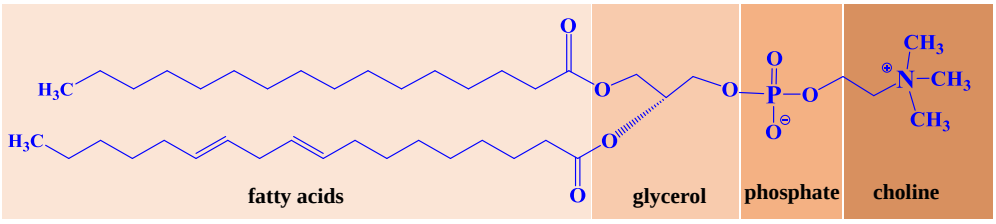

Fig. 1. The molecular structure and functional groups of phosphatidylcholine (PC)

was added dropwise. The solution was then sonicated and heated through an oil bath at different temperatures (room temperature, 40, 60, 80°C). After this, the mixture was centrifuged and the resulting precipitate washed several times with a 1:1 ethanol-distilled water solution. The resulting precipitate was dried in an oven at 60°C for 48h. Finally, the modified bentonite powder was finely ground in an agate mortar. The schematic representation of experimental workflow followed for preparing organo-bentonite is provided in Fig. 2.

Further description of the materials and characterization technique are available in supplementary information (SI).

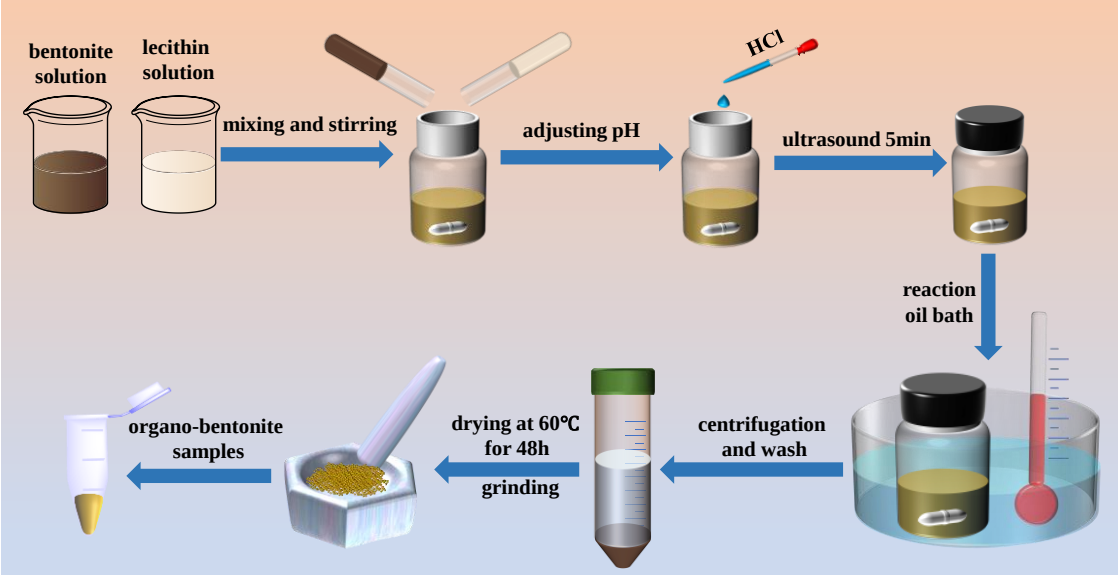

Fig. 2. Schematic representation of the experimental workflow

3. Results and discussion

3.1 Effect of reaction temperature

The effect of reaction temperature on the interlayer space and thermal stability of modified bentonite was studied by a series of experiments with pH=1.0 and 1.0CEC. The XRD patterns of bentonite and modified bentonite prepared at different temperatures were shown in Fig. 3. The bentonite presented a reflection at 2θ=7.28° with a basal spacing d_{001} of 1.21 nm. This reflection shifted to 2θ = 6.15° in the patterns of modified bentonite (room temperature), and the corresponding basal spacing is d_{001} = 1.44 nm, indicating that the lecithin molecules were introduced into the bentonite interlayer space (Songurtekin et al., 2013). Since the TOT layer thickness of montmorillonite is 0.96 nm, the lecithin intercalation increased the interlayer space of sample by 0.48 nm. The intercalation behavior is attributed to the monolayer arrangement of lecithin molecules in the interlayer space (Ouellet-Plamondon et al., 2014). In addition, the XRD results of bentonite modified

with lecithin at different temperatures showed that temperature do not have an effect on the intercalation behavior of lecithin.

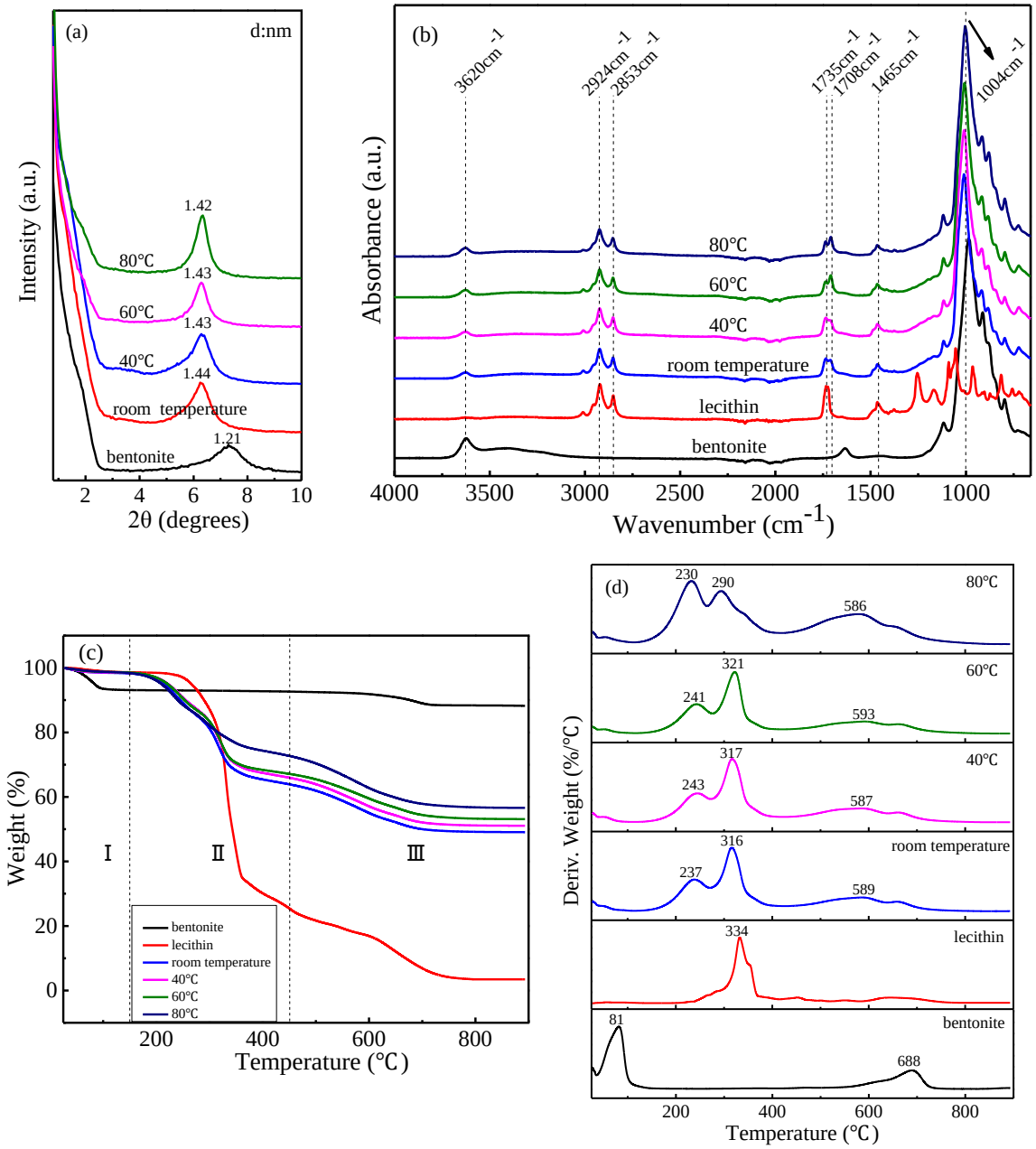

Fig. 3. Top: XRD patterns (a) and FTIR spectra (b) of bentonite, lecithin and modified bentonite at different reaction temperature. Bottom: The TG (c) and DTG (d) curves of bentonite, lecithin and modified bentonite at different reaction temperatures.

FTIR spectroscopy was applied to investigate and compare the functional groups present in raw bentonite, lecithin and modified bentonite. FTIR spectra (Fig. 3) of all

136 modified bentonite samples displayed a band at 3620 cm^{-1} attributed to the -OH
137 stretching vibration of the hydroxyl groups of the bentonite structure. The absorption
138 band centered at around 1004 cm^{-1} is attributed to the Si-O-Si stretching band of
139 bentonite (Xue et al., 2007). The bands at 2924 cm^{-1} and 2853 cm^{-1} are assigned to
140 the -CH_2 asymmetric and symmetric stretching vibrations of the lecithin, respectively
141 (Li et al., 2008; Zhang et al., 2012). An intense band attributed to the C=O group of
142 lecithin occurred at 1735 cm^{-1}, and another one centered at 1465 cm^{-1} belonged to the
143 deformation vibrations of CH_2/CH_3 (Liu et al., 2017; Nagy et al., 2013). The presence
144 of lecithin in the modified bentonite was confirmed by the appearance of the bands
145 centered at 2924 cm^{-1}, 2853 $cm^{-1}$and 1465 cm^{-1}, respectively. The apparent shift of
146 the C=O stretching band at 1735 cm^{-1} in lecithin to 1708 cm^{-1} in modified bentonites
147 indicated possible interactions with the clay layers surface (Merino et al., 2016).

148 Various reports in the literature indicated that thermogravimetric analysis is often
149 used to research the thermal stability of organoclays (Corcione and Frigione, 2012).
150 The way in which the mass loss steps occur provided information on the structure of
151 the intercalated molecules (Xi et al., 2005). The decomposition of bentonite modified
152 with lecithin often occurs in three steps: dehydration of adsorbed water, lecithin
153 decomposition, and silicate dehydroxylation (Zhu et al., 2011).

154 The thermal gravimetric (TG) and differential thermogravimetry (DTG) results
155 for bentonite, lecithin and modified bentonite were compared in Fig. 3 and the lecithin
156 loading amounts were calculated according to the formula in Eq. (1)(Zhu et al., 2017)

157 $$Q_l = \frac{Q_m}{(1-Q_m)\times CEC\times M} \quad (1)$$

where Q_l is the loading amount of lecithin, Q_m is the mass loss in the temperature range of 150~450 °C, M is the molar mass of lecithin. The mass loss results of the modified bentonite and loading amount of lecithin are summarized in Table S1.

In the curve for bentonite (Fig. 3), two major peaks were presented. The first mass loss from the ambient temperature to 150°C and is assigned to dehydration of physisorbed and represent 6.9%. The other mass loss between 450°C and 900°C is attributed to the dehydroxylation of the aluminosilicate layer at 688°C (Khalaf et al., 2017). The mass loss of lecithin mainly occurred between 150 and 450 °C with a mass loss of 73.5%. The temperature corresponding to the highest rate of mass loss was at 334°C for lecithin. These results were in accordance with previous literature reports (Wicklein et al., 2010). Three steps of the mass loss were observed for the organoclays: the first mass loss which is attributed to the dehydration of physisorbed water varied between 1.5% and 1.8%. The most remarkable difference between the bentonite and the organic bentonite is in the temperature range 150~450°C. When the reaction was carried out at room temperature, 40°C, 60°C and 80°C, the second mass loss in the temperature of 150~450℃ was 34.4%, 32.5%, 31.4% and 25.7%, respectively, which is associated with lecithin decomposition (Ouellet-Plamondon et al., 2014). It is found that there are two peaks in this range, the peaks at 200~260, 270~340 °C correspond to the decomposition of the adsorbed surfactant and intercalated surfactant lecithin, respectively. The third mass loss step between 450 to 900 °C is attributed to the dehydroxylation of the structural OH units of the bentonite.

As can be seen from Table S1, with the reaction temperature increase, the mass loss of loaded lecithin decreases from 0.58CEC (for room temperature) to 0.38CEC (for 80℃). This phenomenon occurs because temperature influences the lecithin molecules adsorption capacity.

The macroscale appearance of the organic bentonite samples obtained at different reaction temperature are shown in Fig. S1. There was an obvious difference in appearance characters of organic bentonite samples produced at different temperatures. The organic bentonite samples presented black flake solid at reaction temperature below 60°C, while the sample was the yellowish-brown powder when the temperature was 80°C. The reason for this result may be that temperature affects the adsorption capacity of lecithin molecules on the surface of bentonite. As the temperature increased, the adsorption capacity of lecithin on the bentonite surface decreased, which led to the diminution of the lecithin content in the organic bentonite. Therefore, the appearance of samples changed from black flake solid to yellowish-brown powder. This was also consistent with the TG analysis results.

3.2 Effect of reaction time

The effect of the length of the reaction time on the properties of modified bentonite was also studied. The reaction temperature was set to 60℃. Then, the reaction time was varied from 0.5h to 6.0h.

X-ray diffraction patterns of the modified bentonite at different reaction times were illustrated in Fig. 4. The bentonite showed an interlayer basal spacing of 1.21 nm. After 0.5h of reaction, the X-ray reflection of modified bentonite shifted to a

lower angle and the basal spacing increased from 1.21 to 1.42 nm. This indicated that the intercalation behavior of lecithin molecules was completed at a short time (0.5h). Additionally, the basal spacing d_{001} values (~ 1.42 nm) and reflection intensity did not change for the organo-bentonite samples at different reaction time, which could be attributed to the monolayer arrangement of the lecithin molecules in the interlayer space. This finding indicated that reaction time had no effect on the basal spacing of the modified bentonite. The result has been found to be in good agreement with the literature (Merino et al., 2016).

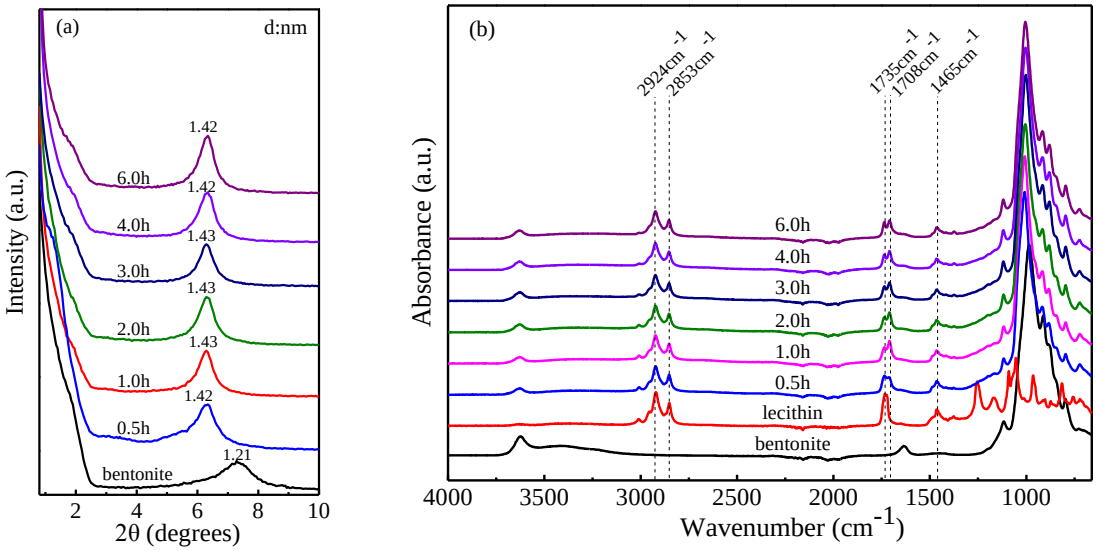

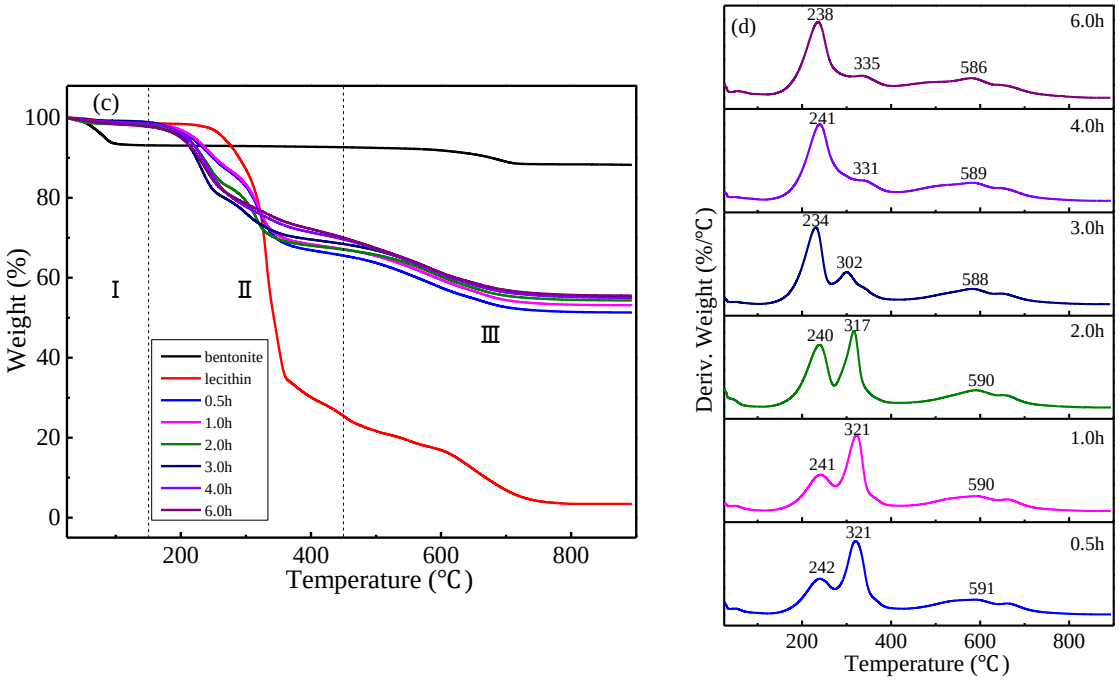

Fig. 4. Top: XRD patterns (a) and FTIR spectra (b) of bentonite, lecithin and modified bentonite at different reaction times. Bottom: The TG (c) and DTG (d) curves of modified bentonite at different reaction times.

The bands in the FTIR spectra were consistent with the ones detailed in the previous section (i.e., the effect of reaction temperature). Upon intercalation with different reaction times, the FTIR experimental results remained consistent. It showed that the reaction time had no influence on the properties of lecithin-modified bentonite, which is agreement with the results of XRD.

The thermal stability of modified bentonite was evaluated by TG analysis and the results of samples were shown in Fig. 4. For modified bentonite, between 150 and 450°C, the mass loss is mainly caused by the lecithin decomposition. Table S2 listed the percentages of mass loss of the different stages and loaded amount of lecithin. The maximum mass loss of lecithin, determined from TG curves, was completed at 0.5h

(32.6%). When the reaction time increased from 0.5h to 6.0h, the mass loss of lecithin decreased from 32.6% to 27.7%, which demonstrated that the lecithin molecules rearrangement were taken place with the increase of reaction time (Merino et al., 2016; Wicklein et al., 2010). The loaded amount of lecithin molecules slightly decreases with the increases of time. This was also evidenced from the appearance of the samples (Fig. S2). The appearance turned from flack solid to powder as the reaction time increase. The DTG of the modified bentonites showed two peaks between 150 and 450 °C, which are attributed to lecithin decomposition. It can be seen from Fig.4, the intensity of the first peak increased with reaction time, whereas the second peak intensity decreased. Changes in the endothermic peak intensity suggested different conformation states and environments of lecithin in the modified bentonite (Silva et al., 2014; Wei Xie, 2001). In addition, organo-bentonites began to decompose at slightly higher temperature with the reaction time increased.

3.3 Effect of pH

The effect of pH on the final performance of modified bentonite was studied. The reaction temperature was set to 60℃ and the reaction time was 1.0h. The pH of the mixture solution was varied from pH=1.0 to pH=9.0.

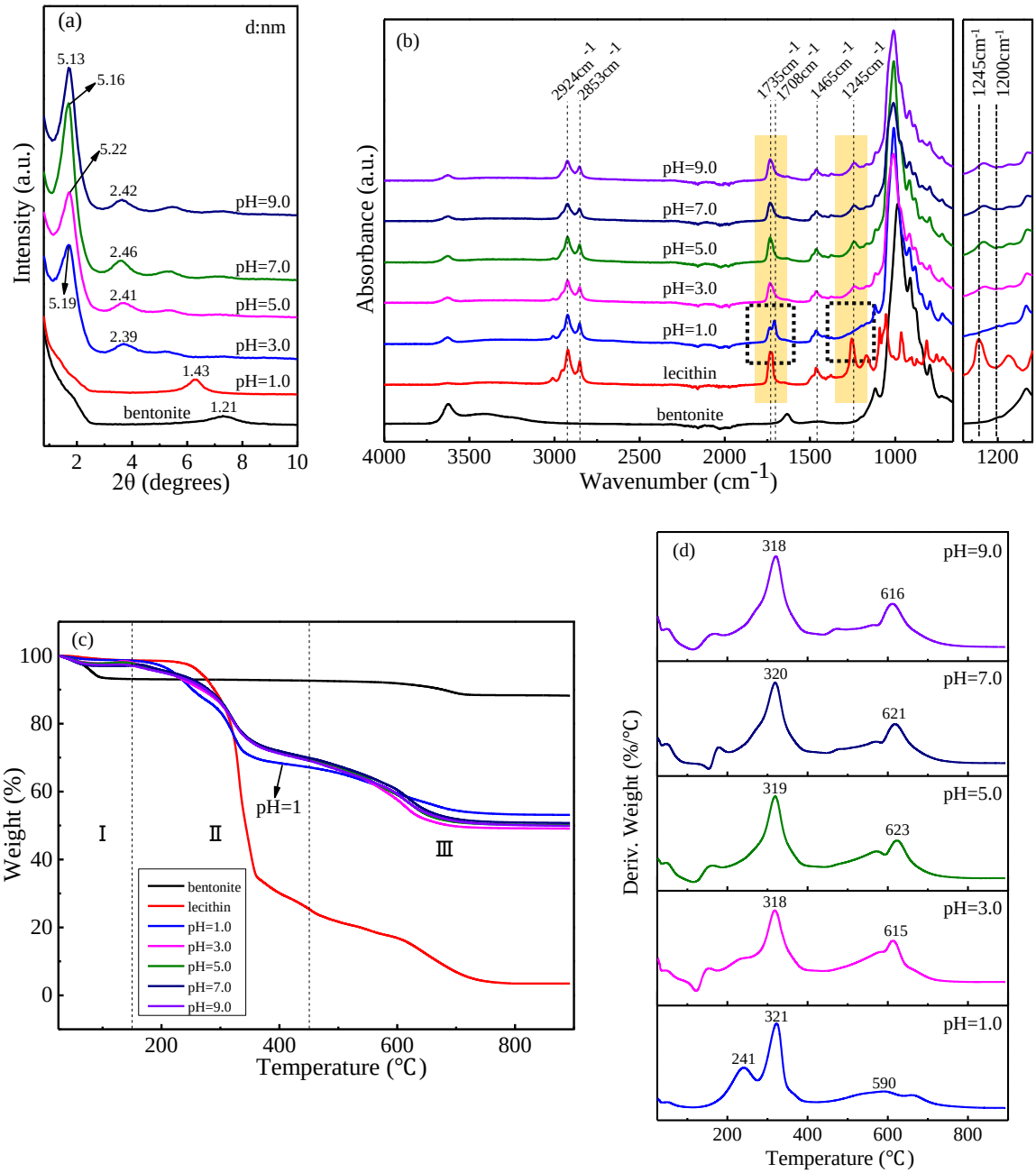

Fig. 5. Top: XRD patterns (a) and FTIR spectra (b) of bentonite, lecithin and modified bentonite at different pH. Bottom: The TG (c) and DTG (d) curves of modified bentonite at different pH.

The XRD patterns of modified bentonites at different pH were presented in Fig. 5. The typical XRD reflections of bentonite related to the basal spacing appeared at 2θ = 7.28° (d_{001} = 1.21 nm). This reflection shifted to 2θ = 6.16° in the patterns of modified bentonite at pH=1.0, corresponding to a d_{001}-value of 1.43 nm. This result

241 was already discussed in the previous sections. At pH=3.0, the basal spacing of the
242 modified bentonite appeared at 2θ = 1.70°, corresponding to the d_{001}-value of 5.19 nm.
243 This showed that when the solution pH reached 3.0, lecithin molecules conformation
244 has changed and the basal spacing was well expanded, increasing from 1.21 to 5.19
245 nm. The (001) reflections of samples at pH=5.0, 7.0, 9.0 appeared at 2θ = 1.69°, 1.71°
246 and 1.72°, corresponding to d_{001}-value of 5.22, 5.16 and 5.13 nm, respectively. In
247 addition, the (002) reflection appears when mixture solution pH exceeds 3.0,
248 indicating that more surfactants were intercalated into the layer, and multiple
249 arrangement models of the lecithin molecule were formed (Zhu et al., 2011). It could
250 be concluded that the pH value of the solution has a great effect on the basal spacing
251 and the intercalation behavior of lecithin.

252 Fig. 5 exhibited the FTIR spectra of modified bentonite under different reaction
253 pH. The bands around 1735 cm^{-1} are attributed to the C=O group of lecithin and the
254 bands at 1245 cm^{-1} is assigned to the PO_2 vibration (Nzai and Proctor, 1998). When
255 pH=1.0, the band assigned to C=O stretching shifts from 1735 cm^{-1} to 1708 cm^{-1}, and
256 the PO_2 vibration shifts from 1245cm^{-1} to 1200 cm^{-1} in modified bentonite. However,
257 when the pH varied from pH=3.0 to pH=9.0, there was no shift of the C=O stretching
258 band and the PO_2 vibration. The protonation of the phosphate group on lecithin is the
259 main reason for this result. The discrepancy reflects the changes of the lecithin
260 properties at different pH conditions. This change is not only directed by the lecithin
261 molecule structure and conformation, but also by interaction with mineral surface.

262 Phosphatidylcholine (PC), which is the main component of lecithin, contains a

choline part that has a negative charge on the phosphate group and a positive charge on the trimethyl-amino group (Fig. 1) (Bot et al., 2021). The pKa value of the phosphate groups PC is around 1.5 (Ogawa et al., 2004). A.J. De Koning and K.B. Mcmullan(De Koning and McMullan, 1965), who investigated the acid hydrolysis of phospholipids, have shown that the oxygen atom in the phosphate group is available for protonation. In a strongly acidic medium(pH<pKa), the phosphate group is protonated, resulting in a positively charged molecule. This change in properties causes different lecithin molecule arrangement, resulting in obvious increase in the interlayer space. The appearance characteristics of the organic bentonite samples indicated that the samples were homogeneous powder when the pH exceeds 3.0 (Fig.S3). The appearance of the samples also reveals the effect of pH on the intercalation behavior of lecithin.

The TG and DTG results for modified bentonite samples at different pH were shown in Fig. 5 and Table S3. When the pH of the solution is 1.0, the maximum mass loss is between 150 and 450°C (31.4%). However, it can be found that, when the pH is higher than 1.0, all the TG curves exhibited similar variation tendencies from room temperature to 900°C, and the amount of lecithin decomposition was around 28.0% and the loaded amount of lecithin was around 0.43CEC between 150 and 450 °C. The corresponding DTG curves in Fig. 5 showed that when pH≥3.0, there were two peaks. The center of the peak was 318°C, corresponding to lecithin decomposition and the center of the peak was 615°C, corresponding to the dehydroxylation of the aluminosilicate layer, respectively. However, when pH=1.0, there was three peaks.

285 The centers of the peaks were 241,321 and 590°C, respectively. Lecithin molecules
286 can exhibit cationic properties due to the protonated choline groups in the highly acid
287 condition (pH=1.0), while display zwitterionic nature when pH≥3.0 (Liu et al., 2017;
288 Ouellet-Plamondon et al., 2014). We have also observed that at pH = 1.0 there are
289 more lecithin molecules absorbed that at pH= 3.0 (Table S3) despite having a smaller
290 d_{001}, i.e. 1.43 vs 5.19 nm. The main reason for this result is the interaction of
291 protonated lecithin with the negatively charged clay surface at pH=1.0. Some
292 surfactant molecules attach to the bentonite surface increased the amount of lecithin,
293 which can be confirmed by a new peak at 241°C for DTG curves.

294 ***3.4 Effect of lecithin concentration***

295 The effect of lecithin concentration on the interlayer space and thermal stability
296 of modified bentonite was studied. The amounts of lecithin selected for the
297 experiment were equivalent to 0.1, 0.5, 1.0, 2.0, and 3.0 times of the bentonite CEC.
298 The pH of the mixture solution was adjusted to pH=1.0, the temperature was set to 60℃
299 and the reaction time was 1.0h.

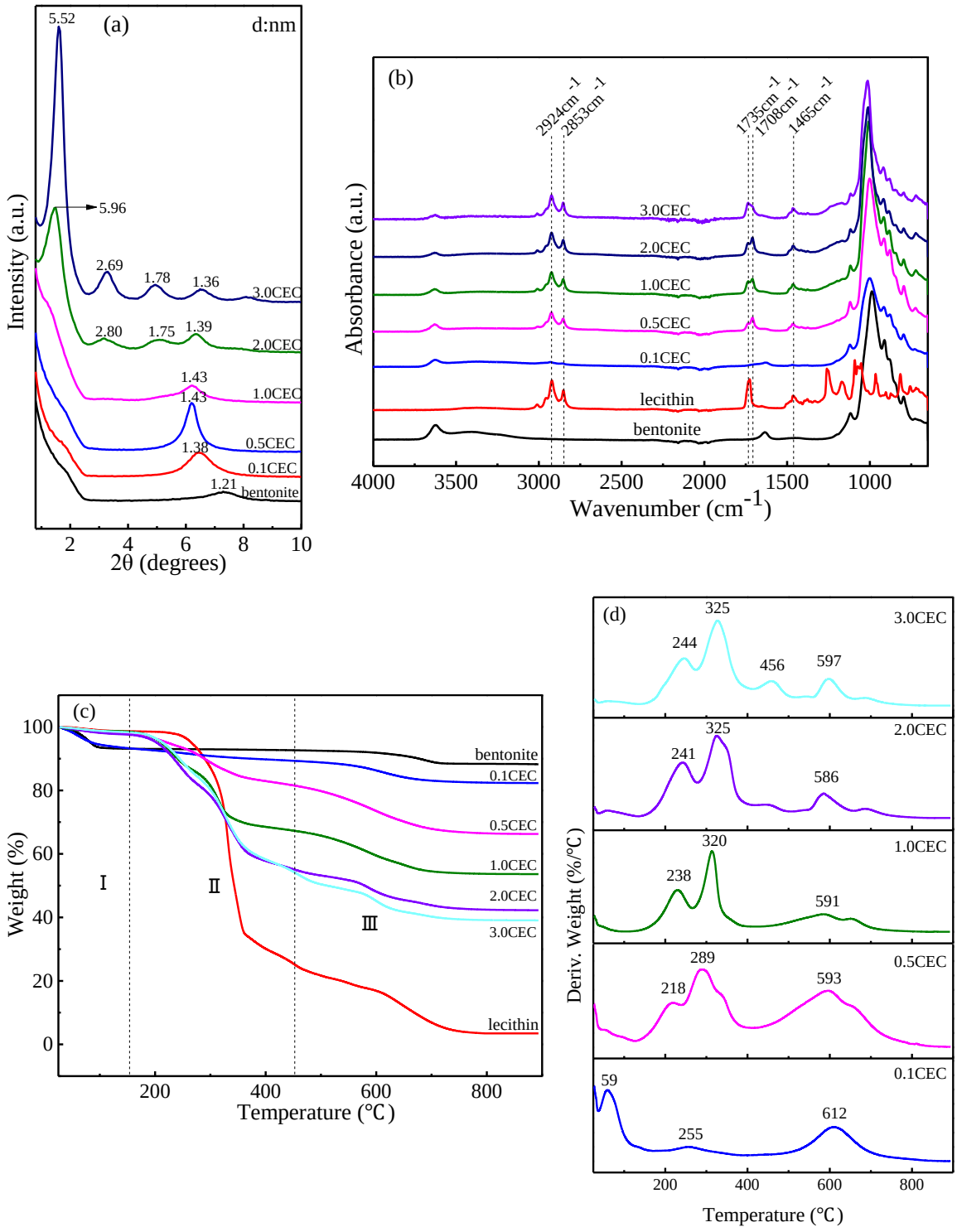

Fig. 6. Top: XRD patterns (a) and FTIR spectra (b) of bentonite, lecithin and modified bentonite at different lecithin concentration. Bottom: The TG (c) and DTG (d) curves of modified bentonite at different lecithin concentration.

300 XRD patterns of the modified bentonite at different lecithin concentration were

illustrated in Fig. 6. The basal spacing d_{001} of bentonite (1.21nm) shifted to 1.38, 1.43, 1.43, 5.96 and 5.52nm after modification with 0.1, 0.5, 1.0, 2.0 and 3.0CEC, respectively. When the lecithin concentration was between 0.1 and 1.0 CEC, the d_{001} reflection increased slightly from 1.38 to 1.43 nm, which is correspond to lateral monolayer arrangement of the lecithin molecule. From 2.0 to 3.0 CEC, lecithin expanded the bentonite basal spacing d_{001} up to nearly 5.52nm, which hold an interlayer space of 4.56nm (after subtraction of the TOT layer thickness value of 0.96 nm). These results indicated that the lipid bilayer adopt a different conformation in the interlayer space (Fig. 7). In regards to the length of one PC molecule (about 3nm) we can imagine that PC molecules are now perpendicular to the clay surface in an upright position. In addition, when the lecithin concentration is increased from 2.0 to 3.0 CEC, the 001 reflections turn to be much shaper and intensity become much higher, which suggested that the lecithin molecules arrangement in the clay layers were more ordered.

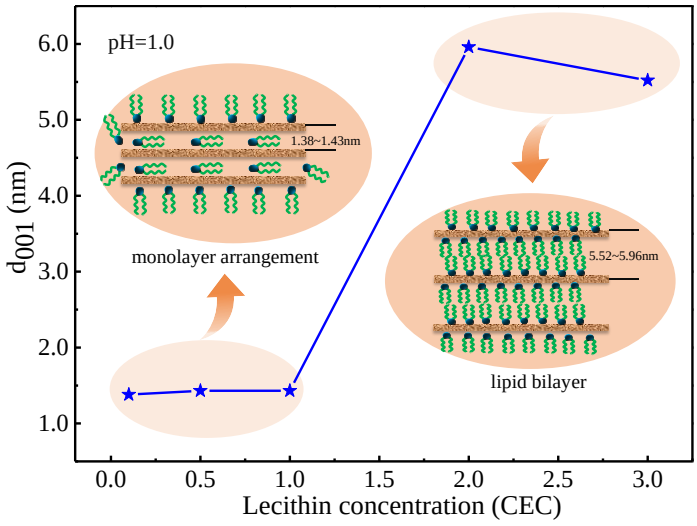

Fig. 7. Schematic diagram of the lecithin arrangement in the interlayer space at different

concentration.

For organic bentonite modified with 0.5, 1.0, 2.0CEC, the elemental composition of the samples were determined by XRF analysis, obtaining data in Table 1. The raw bentonite had alumina and silica as the major species, at 22.9% and 65.1% by weight, respectively. Na^+ and Ca^{2+} are the main exchangeable cation of bentonite. It was found that P_2O_5 were present in organic bentonite at 3.59%(0.5CEC), 6.17%(1.0CEC) and 11.4%(2.0CEC), respectively. This implies that the intercalation of lecithin molecules was successful by ion exchange. In addition, the experimental results suggest obvious decreases in the cations of the interlayer (Na^+, Ca^{2+}), which confirms that cation exchange and replacement are the mechanisms of action in the modification process.

Table 1. Chemical composition of raw bentonite and organic bentonite measured by XRF.

lecithin concentration /CEC	chemical composition (mass%)								
	Na_2O	MgO	CaO	K_2O	Al_2O_3	SiO_2	Fe_2O_3	P_2O_5	other
0 (raw bentonite)	2.56	2.84	1.23	0.32	22.9	65.1	4.22	0.06	0.77
0.5	0.31	2.32	0.42	0.30	23.1	64.9	4.74	3.59	0.24
1.0	0.21	2.51	0.29	0.24	22.7	63.6	4.04	6.17	0.26
2.0	0.15	2.30	0.32	0.24	21.3	60.1	3.97	11.4	0.24

For a better understanding of the morphology of organoclays, TEM micrographs of raw bentonite and the obtained organoclays are presented in Fig. 8. The micrograph of raw bentonite (left picture) suggested that the untreated bentonite is mainly composed of a layered structure with a $d_{(001)}$ measured = 1.2 nm, in good agreement with the value obtained by XRD analysis. The second micrograph of organoclay modified with 1.0CEC lecithin (middle picture) clearly displayed an increase in the

interlayer spacing compared to raw bentonite. Finally, for organic bentonite modified with 2.0CEC lecithin (right picture), multiple interlayer spacings are observed at 5.8, 1.7, and 1.4 nm, slightly smaller than the XRD measured d_{001}-value of 5.96 nm. Indeed, XRD results corresponds to an average value while TEM measurements are based on individual layers.

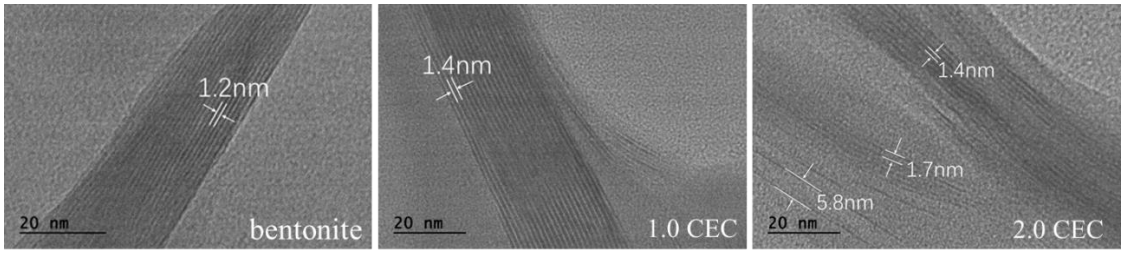

Fig. 8. TEM micrographs of raw bentonite and organoclays modified with lecithin at different lecithin concentration.

The peaks that appeared in the FTIR spectra were consistent with the ones detailed in the previous section (i.e., the effect of reaction temperature). The absorption peak intensity of samples increased as a function of the lecithin concentration, indicating that more lecithin was adsorbed onto the clay surface and intercalated into the interlayer of bentonite. It can be seen from Fig. S4 that the sample color was getting darker and gradually changing from powder to flake solid. This was mainly caused by the excessive loading of lecithin on the bentonite.

TG and DTG results also hint at a larger number of intercalated at higher lecithin concentrations (Table S4). The mass loss between 150°C and 450°C goes from 4.0% to 43.5% when the lecithin concentration is between 0.1 and 3.0CEC. For bentonite modified with 0.1CEC, the first degradation peak was observed at around 59°C, with a 6.7% mass loss assigned to the evaporation of the adsorbed water. When the

temperature was between 150 and 450 °C, the sample exhibited only one degradation peaks at 255 °C, which can be attributed to the decomposition of intercalated lecithin molecules. The thermal decomposition stages for the 0.5CEC sample are similar to those for the 1.0CEC and 2.0CEC sample with DTG peaks (Fig. 6). But when the temperature varied between 150 and 450°C, the degradation temperature of samples shifted to a higher temperature with the lecithin concentration increased, which displays a further enhancement in the thermal stability. With the increase in surfactant concentration, a new endothermic peak appeared at ~456 °C for 3.0CEC. This step could be ascribed to the presence of triglycerides and other impurity, which is consistent with the already published literature(Ouellet-Plamondon et al., 2014).

In order to have a deeper understanding of the physiochemical processes of organic matter and clay minerals at the microscopic level, classical molecular dynamic (MD) simulations have been proven to be an effective method to obtain structural information among the constituents (Kovar et al., 2010). We have modelled the system at pH=1.0, 60°C and when a PC concentration regarding the CEC of 2.0 was added. The calculation details are available in supplementary information(SI).

Five molecular dynamics simulations (MD) of 10 ns were performed on a small slab of montmorillonite, composed of 9×9×2 (x,y,z) unit cells. At first all PC molecules are added directly inside the interlayer space of the clay randomly, the exact number is related to the experimental loading amount measured.

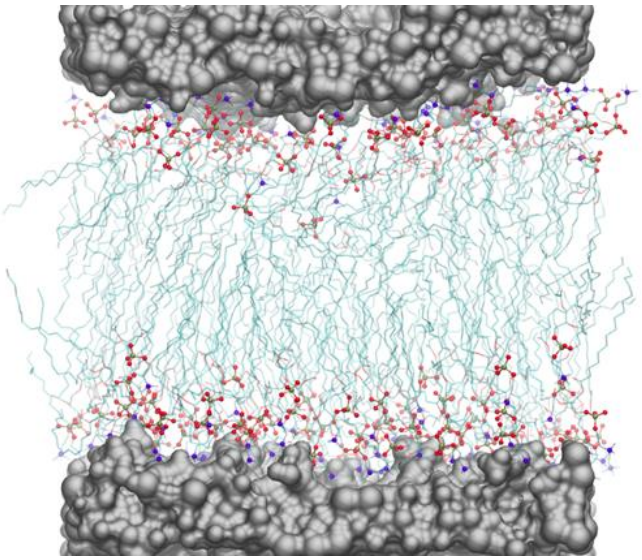

Fig. 9. Snapshot of the last step of the MD3. The N and PO_4 group of the PC molecules are highlighted using ball representation. The montmorillonite surface is represented by a gray surface with a probe radius of 1 A. The color code used is the following: blue N, red O, gold P, green C.

Table 2. Computed d_{001} at the last step of the related MD and percentage of N (from amine) or OH (from phosphate) of the PC molecules in interaction with the surface at a distance of 0.68 nm.

MD number	1	2	3	4	5
Computed d_{001} (in nm)	6.214	6.14	6.029	6.02	6.33
%N (amine) in interaction with the surface	94%	91%	91%	92%	92%
%OH (phosphate) in interaction with the surface	69%	63%	66%	62%	66%

From these dynamics results, we can draw some conclusions (Fig. 9). First we will discuss about the PC absorption. We have observed that the PC auto-organized themselves quickly, even before the MD production. The amine head points in the direction of the T layer of the montmorillonite. However, it is often not directly in interaction with this one, but in most cases, involved in a hydrogen bond network with a water molecule in between the clay structure and the PC. The second type of interaction comes from the OH group of the phosphate which is protonated at pH=1.0. It is either directly bonded to the oxygen atom of the T sheet of the Mt or through a

water molecule. In Table 2, we have printed the percentage of nitrogen (from the amine group) or O (from the OH group of the phosphate) in interaction with the surface *i.e.* below 0.68 nm. This distance corresponds to the sum of the Van der Waals radius of either the amine group, a water molecule and an oxygen of the silicate or the OH group of the phosphate, a water molecule and an oxygen of the silicate. For all MDs more than 90% of the lecithin molecules are in interaction with the surface. However some of them do not interact at all and instead in interaction with other PC. Finally, once the PC is in interaction with the montmorillonite, no major displacements are observed during the MD. This tends to validate the experimental observations where the PC is strongly absorbed in the interlayer space at 60°C.

Let's now focus in the orientation of the PC tails in the interlayer space. The PC molecule optimized in vacuo using DFT calculations has a length of 3 nm (from a carbon of the amine group to the last carbon of the tail). In comparison to the maximum interlayer space measured (4.56 nm when removing the TOT distance), 2 PC molecules cannot fit inside the interlayer space without some bending. In the Fig. S5, we have represented several possible organizations of the PC molecules. They can adopt a lot of different conformation, some are nearly linear while others are heavily bended. On top of this, several PC (green, orange in Fig. S5) interact with the surface with both amine and phosphate groups but also with the oxygen atoms of the linear chains. In the end, the disposition of PC molecules is relatively random, maybe due to the short time of the simulation.

Finally we also analyzed the distance of the interlayer space during the MD. As

404 written before the PC tends to self-organized very quickly, and after 4 ns the stable
405 regime is observed regarding the total energy of the system. For each MD, the relative
406 distance of the interlayer space is reported in Table 2 and taken from the last step of
407 the simulation. It is difficult to give a precise number as the TOT layers of the
408 montmorillonite are slightly altered by the MD due to not being constrained. In any
409 case, for the 5 MDs the computed d_{001} distance reproduced accurately the measured
410 one with a maximum deviation of 6 %. One of the reasons could be that we have
411 added too many PC molecules in the interlayer space. As written before 5 to 10 % of
412 PC molecules are not in interaction with the clay, and instead are freely moving in the
413 interlayer space, disrupting the local order.

414 ***Conclusions***

415 In this study, a series of organo-bentonites were synthesized by using natural
416 soybean lecithin at different experimental conditions. The effects of reaction
417 temperature, time, pH, and lecithin concentration on the properties of modified
418 bentonite were analyzed. The results of FTIR, XRD, TG and molecular dynamic
419 simulations support the intercalation of lecithin in the interlayer space of
420 montmorillonite. The characterization results demonstrate that the intercalation
421 behavior of lecithin can be completed in a short time (0.5h). Lecithin concentration
422 and pH greatly influence the structural characteristic of modified bentonite. In general,
423 the basal spacing of the organo-bentonite has a positive correlation with lecithin
424 concentration and pH. In the case of pH=1.0, the interlayer spacing of modified
425 bentonite increases with the lecithin concentration and the surfactants exhibit different

arrangements among the bentonite layers. Lecithin adopts a lateral monolayer arrangement at low concentrations (0.1~1.0CEC) in contrary to a lipid bilayer at high concentrations (2.0~3.0CEC), this last one being perpendicular to the surface. Regarding the effect of the pH , the d_{001} of the bentonite layer was significant higher for the samples prepared at pH≥3.0 due to the properties change of both the surface and the lecithin. For example, when the pH shifts from 1.0 to 3.0, the interlayer spacing of organoclay was increased from 1.43 to 5.19 nm, which is of great significance for the preparation of low-cost organobentonite for industrial applications. These results demonstrate that the modified bentonite with lecithin have quite different structural properties, and they may have special applications in the industrial fields.

Acknowledgments

Qiang Li is grateful for the scholarship (No. 202006440010) awarded by the China Scholarship Council (CSC).

References

Agwu, O.E., Akpabio, J.U., Ekpenyong, M.E., Inyang, U.G., Asuquo, D.E., Eyoh, I.J., Adeoye, O.S., 2021. A critical review of drilling mud rheological models. Journal of Petroleum Science and Engineering 203, 108659.

Bergaya, F., and Gerhard Lagaly, 2013. Handbook of clay science. Newnes.

Bergaya, F., Lagaly, G., 2006. Chapter 1 General Introduction: Clays, Clay Minerals, and Clay Science, in: Bergaya, F., Theng, B.K.G., Lagaly, G. (Eds.), Developments in Clay Science. Elsevier, pp. 1-18.

448 Biswas, B., Warr, L.N., Hilder, E.F., Goswami, N., Rahman, M.M., Churchman, J.G., Vasilev,
449 K., Pan, G., Naidu, R., 2019. Biocompatible functionalisation of nanoclays for improved
450 environmental remediation. Chemical Society Reviews 48, 3740-3770.
451 Bot, F., Cossuta, D., O'Mahony, J.A., 2021. Inter-relationships between composition,
452 physicochemical properties and functionality of lecithin ingredients. Trends in Food Science &
453 Technology 111, 261-270.
454 Churchman, G.J., Gates, W.P., Theng, B.K.G., Yuan, G., 2006. Chapter 11.1 Clays and Clay
455 Minerals for Pollution Control, Handbook of Clay Science, pp. 625-675.
456 Corcione, C.E., Frigione, M., 2012. Characterization of Nanocomposites by Thermal Analysis.
457 Materials 5, 2960-2980.
458 Cui, J., Wang, Q., Chen, X., Wei, Q., 2014. A novel material of cross-linked styrylpyridinium
459 salt intercalated montmorillonite for drug delivery. Nanoscale Res Lett 9, 378-378.
460 Cui, L., Decker, E.A., 2016. Phospholipids in foods: prooxidants or antioxidants? J Sci Food
461 Agric 96, 18-31.
462 De Koning, A.J., McMullan, K.B., 1965. Hydrolysis of phospholipids with hydrochloric acid.
463 Biochimica et Biophysica Acta (BBA) - Lipids and Lipid Metabolism 106, 519-526.
464 Dening, T.J., Rao, S., Thomas, N., Prestidge, C.A., 2017. Montmorillonite-lipid hybrid carriers
465 for ionizable and neutral poorly water-soluble drugs: Formulation, characterization and in vitro
466 lipolysis studies. International Journal of Pharmaceutics 526, 95-105.
467 Khalaf, A.I., Hegazy, M.A., El-Nashar, D.E., 2017. Synthesis and characterization of cationic
468 gemini surfactant modified Na–bentonite and its applications for rubber nanocomposites.
469 Polymer Composites 38, 396-403.

Kovar, P., Pospisil, M., Kafunkova, E., Lang, K., Kovanda, F., 2010. Mg-Al layered double hydroxide intercalated with porphyrin anions: molecular simulations and experiments. J Mol Model 16, 223-233.

Le, N.T.T., Cao, V.D., Nguyen, T.N.Q., Le, T.T.H., Tran, T.T., Hoang Thi, T.T., 2019. Soy Lecithin-Derived Liposomal Delivery Systems: Surface Modification and Current Applications. 20, 4706.

Li, S., Mu, B., Wang, X., Wang, A., 2021. Recent researches on natural pigments stabilized by clay minerals: A review. Dyes and Pigments 190.

Li, Z., Jiang, W.T., Hong, H., 2008. An FTIR investigation of hexadecyltrimethylammonium intercalation into rectorite. Spectrochim Acta A Mol Biomol Spectrosc 71, 1525-1534.

Lima, L.C.B., Silva, F.C., Silva-Filho, E.C., Fonseca, M.G., Zhuang, G., Jaber, M., 2020. Saponite-anthocyanin derivatives: The role of organoclays in pigment photostability. Applied Clay Science 191.

Liu, S., Wu, P., Yu, L., Li, L., Gong, B., Zhu, N., Dang, Z., Yang, C., 2017. Preparation and characterization of organo-vermiculite based on phosphatidylcholine and adsorption of two typical antibiotics. Applied Clay Science 137, 160-167.

Makhoukhi, B., Villemin, D., Didi, M.A., 2013. Preparation, characterization and thermal stability of bentonite modified with bis-imidazolium salts. Materials Chemistry and Physics 138, 199-203.

Makhoukhi, B., Villemin, D., Didi, M.A., 2016. Synthesis of bisimidazolium–ionic liquids: Characterization, thermal stability and application to bentonite intercalation. Journal of Taibah University for Science 10, 168-180.

492 Merino, D., Ollier, R., Lanfranconi, M., Alvarez, V., 2016. Preparation and characterization of
493 soy lecithin-modified bentonites. Applied Clay Science 127-128, 17-22.
494 Nagy, K., Bíró, G., Berkesi, O., Benczédi, D., Ouali, L., Dékány, I., 2013. Intercalation of
495 lecithins for preparation of layered nanohybrid materials and adsorption of limonene. Applied
496 Clay Science 72, 155-162.
497 Nzai, J.M., Proctor, A., 1998. Determination of phospholipids in vegetable oil by fourier
498 transform infrared spectroscopy. Journal of the American Oil Chemists' Society 75,
499 1281-1289.
500 Ogawa, S., Decker, E.A., McClements, D.J., 2004. Production and Characterization of O/W
501 Emulsions Containing Droplets Stabilized by Lecithin − Chitosan − Pectin Mutilayered
502 Membranes. J. Agric. Food Chem 52, 3595-3600.
503 Ouellet-Plamondon, C.M., Stasiak, J., Al-Tabbaa, A., 2014. The effect of cationic, non-ionic
504 and amphiphilic surfactants on the intercalation of bentonite. Colloids and Surfaces A:
505 Physicochemical and Engineering Aspects 444, 330-337.
506 Park, Y., Ayoko, G.A., Horvath, E., Kurdi, R., Kristof, J., Frost, R.L., 2013. Structural
507 characterisation and environmental application of organoclays for the removal of phenolic
508 compounds. J Colloid Interface Sci 393, 319-334.
509 Pereira, F.A.R., Sousa, K.S., Cavalcanti, G.R.S., França, D.B., Queiroga, L.N.F., Santos,
510 I.M.G., Fonseca, M.G., Jaber, M., 2017. Green biosorbents based on chitosan-montmorillonite
511 beads for anionic dye removal. Journal of Environmental Chemical Engineering 5, 3309-3318.
512 Ruiz-Hitzky, E., Darder, M., Wicklein, B., Castro-Smirnov, F.A., Aranda, P., 2019.
513 CLAY-BASED BIOHYBRID MATERIALS FOR BIOMEDICAL AND PHARMACEUTICAL

APPLICATIONS. Clays and Clay Minerals 67, 44-58.

Sabzevari, A.G., Sabahi, H., Nikbakht, M., McInnes, S.J.P., 2022. Development and characteristics of layered EGCG/Montmorillonite hybrid: An oral controlled-release formulation of EGCG. Journal of Drug Delivery Science and Technology 76, 103750.

Silva, I.A., Sousa, F.K.A., Menezes, R.R., Neves, G.A., Santana, L.N.L., Ferreira, H.C., 2014. Modification of bentonites with nonionic surfactants for use in organic-based drilling fluids. Applied Clay Science 95, 371-377.

Songurtekin, D., Yalcinkaya, E.E., Ag, D., Seleci, M., Demirkol, D.O., Timur, S., 2013. Histidine modified montmorillonite: Laccase immobilization and application to flow injection analysis of phenols. Applied Clay Science 86, 64-69.

Trigueiro, P., Pedetti, S., Rigaud, B., Balme, S., Janot, J.M., Dos Santos, I.M.G., Gougeon, R., Fonseca, M.G., Georgelin, T., Jaber, M., 2018. Going through the wine fining: Intimate dialogue between organics and clays. Colloids Surf B Biointerfaces 166, 79-88.

Wei Xie, Z.G., Wei-Ping Pan, Doug Hunter, Anant Singh, and Richard Vaia, 2001. Thermal Degradation Chemistry of Alkyl Quaternary Ammonium Montmorillonite. Chemistry of Materials 13, 2979-2990.

Wicklein, B., Darder, M., Aranda, P., Ruiz-Hitzky, E., 2010. Bio-organoclays based on phospholipids as immobilization hosts for biological species. Langmuir 26, 5217-5225.

Xavier, K.C.M., Santos, M.S.F., Osajima, J.A., Luz, A.B., Fonseca, M.G., Silva Filho, E.C., 2016. Thermally activated palygorskites as agents to clarify soybean oil. Applied Clay Science 119, 338-347.

Xi, Y., Martens, W., He, H., Frost, R.L., 2005. Thermogravimetric analysis of organoclays

intercalated with the surfactant octadecyltrimethylammonium bromide. Journal of Thermal Analysis and Calorimetry 81, 91-97.

Xie, W., Gao, Z., Liu, K., Pan, W.-P., Vaia, R., Hunter, D., Singh, A., 2001. Thermal characterization of organically modified montmorillonite. Thermochimica Acta 367-368, 339-350.

Xie, W., Xie, R., Pan, W.-P., Hunter, D., Koene, B., Tan, L.-S., Vaia, R., 2002. Thermal Stability of Quaternary Phosphonium Modified Montmorillonites. Chemistry of Materials 14, 4837-4845.

Xue, W., He, H., Zhu, J., Yuan, P., 2007. FTIR investigation of CTAB-Al-montmorillonite complexes. Spectrochim Acta A Mol Biomol Spectrosc 67, 1030-1036.

Zhang, H., Zhang, J., Gao, Y., Wang, W., Dong, H., Hou, H., Liu, X., 2017. Effect of modification extent of montmorillonite on the performance of starch nanocomposite films. 69, 1700088.

Zhang, Y., Zhao, Y., Zhu, Y., Wu, H., Wang, H., Lu, W., 2012. Adsorption of mixed cationic-nonionic surfactant and its effect on bentonite structure. Journal of Environmental Sciences 24, 1525-1532.

Zhou, D., Zhang, Z., Tang, J., Wang, F., Liao, L., 2016. Applied properties of oil-based drilling fluids with montmorillonites modified by cationic and anionic surfactants. Applied Clay Science 121-122, 1-8.

Zhu, J., Qing, Y., Wang, T., Zhu, R., Wei, J., Tao, Q., Yuan, P., He, H., 2011. Preparation and characterization of zwitterionic surfactant-modified montmorillonites. J Colloid Interface Sci 360, 386-392.

Zhu, J., Zhang, P., Qing, Y., Wen, K., Su, X., Ma, L., Wei, J., Liu, H., He, H., Xi, Y., 2017. Novel intercalation mechanism of zwitterionic surfactant modified montmorillonites. Applied Clay Science 141, 265-271.

Zhuang, G., Zhang, Z., Fu, M., Ye, X., Liao, L., 2015. Comparative study on the use of cationic–nonionic-organo-montmorillonite in oil-based drilling fluids. Applied Clay Science 116-117, 257-262.

Zhuang, G., Zhang, Z., Jaber, M., 2019. Organoclays used as colloidal and rheological additives in oil-based drilling fluids: An overview. Applied Clay Science 177, 63-81.